

Simbol-X: x-ray baffle for stray-light reduction.

G. Cusumano^a, M. A. Artale^a, T. Mineo^a, V. Teresi^a, G. Pareschi^b, V. Cotroneo^b

^aINAF-IASF-Pa, via Ugo La Malfa 153, 90146 Palermo, Italy

^bINAF Osservatorio Astronomico di Brera Via E. Bianchi 46 - 23807 Merate (Lc) - ITALY

ABSTRACT

Simbol-X, an hard X-ray mission proposed by a consortium of European laboratories, will operate on a broad energy range (0.5-70 keV) providing a large collecting area ($\sim 1500 \text{ cm}^2$ at 1.5 keV and $\sim 450 \text{ cm}^2$ at 30 keV) and a good imaging capability over the entire energy range. Relying on two spacecrafts in a formation flight configuration, Simbol-X will use, for the first time, a 20 meters focal length X-ray concentrator with multilayers coated mirrors that efficiently focalize photons above 10 keV and enhance the sensitivity up to 70 keV.

Thanks to a ray-tracing code, we simulated the Simbol-X optics performance and investigated the contamination at the focal plane caused by stray-light from diffuse cosmic X-ray background. A dedicated X-ray baffle is mandatory to minimize this contamination that otherwise, would strongly affect the telescope sensitivity. In this paper we investigate different X-ray baffle designs and show their efficiency in reducing the stray-light.

Keywords: X-ray telescopes, X-ray optics, Grazing incidence optics

1. INTRODUCTION

The study of the emission from galactic and extragalactic sources at energies greater than 10 keV is hampered by the moderate sensitivity and spatial resolution of the previous and present missions dedicated to the observations of the hard X-ray sky. Astrophysical missions like Einstein,¹ Rosat,² BeppoSAX,³ ASCA,⁴ XMM-Newton,⁵ Chandra,⁶ Swift⁷ and Suzaku,⁸ thanks to focusing optics based on grazing incident mirrors, have provided better and better spatial resolution and sensitivity in the 0.2-10 keV range. They exploit the total reflection phenomenon at grazing angles up to a critical angle, beyond which the reflectivity rapidly falls down. Above 10 keV angles useful for reflection become very small because of the decreasing of the critical angle with energy. On the other hand, the slope of a mirror at a given distance from the optical axis is tied to the telescope focal length: the shorter is the focal length the larger are the mirror slopes. This determines, as a consequence, a strong limitation of the available collecting area at high energies for optics with usual focal lengths ($< 10 \text{ m}$). Larger focal lengths are therefore mandatory in order to focus harder X-ray. Spacecraft lodging, on the other hand, has limited the focal length of telescope concentrators to only a few meters (7.5 m for XMM-Newton) imposing an energy limit around 10 keV.

Hard X-ray and gamma ray sky images can also be obtained with coded mask imagers⁹ that record the shadow of a mask containing a transparent/opaque pattern, projected onto the detector by all emitting sources of a large region of sky. Coded mask imagers are currently on board of the high energy observatories INTEGRAL¹⁰ and Swift.⁷ In contrast to a focusing imaging telescope, the Point Spread Function of coded mask imagers is spread over the entire detector. By knowing the orientation of the satellite in space and by using complex deconvolution methods it is possible to determine the position and the intensity of the gamma-ray sources, and thus to reproduce the image of the observed sky. The main advantage of the coded mask imagers with respect to the focusing telescopes is that they allow the observation and simultaneous monitoring of a large region of the sky. The disadvantage is that the reconstruction of the intensity, at a particular point in the Field of View (FoV), involves harvesting photons from the entire detector. The detector has to be large, therefore no concentration takes place and, as a consequence, the level of the background and its associated noise result to be very large. Therefore, coded mask imagers produce a much lower signal to noise ratio than the grazing reflection technique which concentrates radiation from a large area onto a small detector. Moreover, they do not allow to reach an

Send correspondence to G.Cusumano

G. Cusumano: E-mail: giancarlo.cusumano@ifc.inaf.it, Telephone: +39 091 6809479

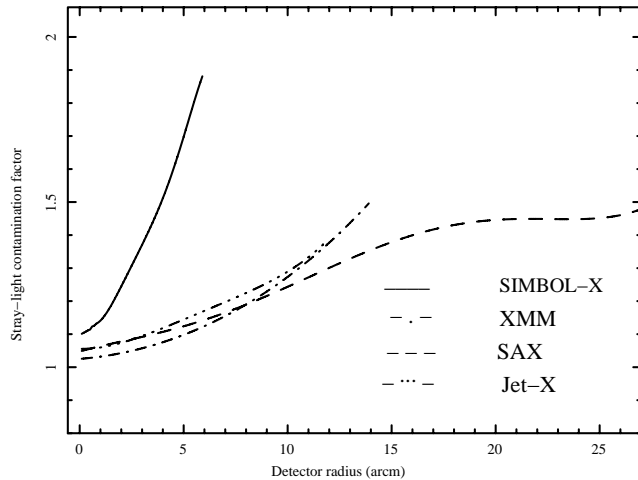


Figure 1. The Simbol-X "stray-light contamination factor" versus the focal plane detector radius. The contamination is compared with that computed for SAX, JET-X and XMM.

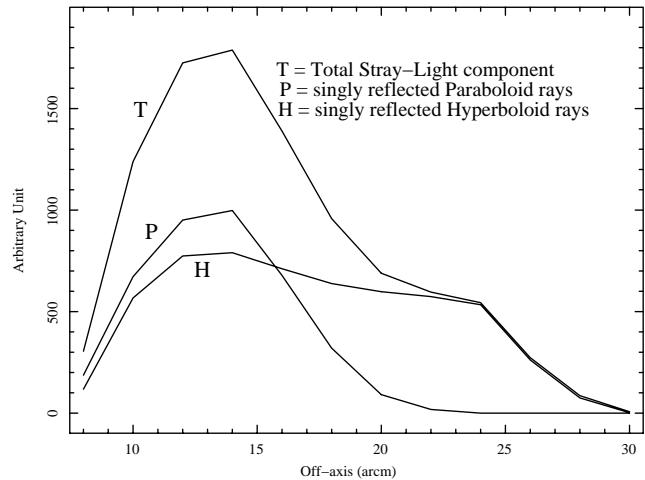


Figure 2. Stray-light originated from X-ray diffuse background emitted from annular regions out of the FoV versus off-axis angles. The entire (T) and the single contributions (P, H) are shown.

angular resolution better than few arc-minutes and they have sensitivity two order of magnitude worse than the concentrators.

Simbol-X¹¹ is a planned hard X-ray mission (0.5–70 keV) aimed to bridge the gap in sensitivity between the two different techniques by extending the X-ray focusing technique to much higher energies. Simbol-X will make use of a grazing incident mirrors telescope with 100 co-axial shells and a focal length of 20 m. The reflectivity efficiency will be enhanced at high energies by the use of multilayers coated mirrors, that, thanks to the Bragg diffraction phenomenon, are characterized by a good reflectivity in an energy range wider than the one achievable with single layers. Multilayers will be deposited on top of a Wolter I configuration mirror structure 0.3-0.1 mm thick, made with the Nickel electroforming technique.¹² The focal plane detector system will combine a Silicon low energy detector, efficient up to ~ 20 keV, on top of a Cd(Zn)Te high energy detector, both surrounded by an active anti-coincidence shield detector. Since the large focal length cannot fit in a single spacecraft, the mirrors and detectors will be flown on two separate spacecrafts in a formation flight configuration.¹³ Thanks to a very large aperture diameter, similar to the XMM mirror module, Simbol-X will allow us to achieve a gain of roughly two orders of magnitude in sensitivity with respect to the present coded mask imagers, maintaining an angular resolution comparable to the current focusing instrument. The mirrors in the Simbol-X telescope will have smaller slopes than mirrors in previous focusing telescopes and the shells location inside the telescope will have large gaps to enhance the effective area at higher energies and minimize the vignetting. The drawback of a telescope with larger than optimum gap between adjacent mirrors is an increase of the stray-light: the contamination by X-ray sources and/or by the diffuse X-ray light background located outside the Simbol-X FoV (6–7 arcmin) whose light goes through the nested concentric mirrors and arrives onto the focal plane detector without undergoing the focusing double reflection. This undesirable light could decrease the sensitivity of the telescope limiting its performance for very faint and/or extended sources. A careful study through a simulation code has been performed to evaluate the stray-light contamination. This paper shows the efficiency of three different X-ray baffle designs dedicated to the minimization of the stray-light contamination and verifies that the performance of Simbol-X telescope is not significantly degraded, because of the implementation of such a baffle, in terms of effective area and vignetting.

2. SIMBOL-X OPTICS SIMULATOR DESCRIPTION

The Simbol-X optics performance has been evaluated by using an "ad hoc" ray-tracing Montecarlo code. The telescope has been modeled on the baseline design made up of 100 nested Wolter-I shaped mirror shells and a focal length of 20 m.¹³ All the optics shells are co-axial and kept together at the entrance and the exit pupils

by a spider structure that reduces the effective area by a factor 0.1. The photon reflection efficiency is computed for a multilayer coated mirror composed of 250 bilayers of carbon and platinum, alternately deposited onto a nickel substrate.¹² The simulation follows the history of each photon from the telescope entrance pupil, along its course through the mirror shells and, if the photon is not absorbed, up to the focal plane. Scattering processes due to surface microroughness on the mirror surface have been included. The response of a detector at the focal plane has not yet been implemented. The code allows to simulate either monochromatic light or photons sorted out from a power law distribution of energies, either point-like or extended spatially uniform X-ray sources.

3. STRAY LIGHT CONTAMINATION

The correct path of the X-ray photons inside an X-ray grazing incident telescope is a double reflection on the mirror surfaces: a first reflection by the paraboloid followed by a second reflection by the hyperboloid. Not all photons at the entrance pupil of the telescope have this focusing double reflection. Some rays, called stray-light, could¹⁴:

- not be reflected by the inner mirror surface at all (*not reflected rays* (**N**)).
- be reflected by the paraboloid but not by the hyperboloid (*singly reflected paraboloid rays* (**P**)).
- not be reflected by the paraboloid but by the hyperboloid only (*singly reflected hyperboloid rays* (**H**)).

Contamination by stray-light is particularly severe for telescopes with large gaps between mirrors. If, because of the stray-light, too many photons from outside the nominal FoV arrive at the focal camera, we have a significant decrease of the sensitivity of the telescope, limiting its performance especially for faint and/or extended sources.

The main effects due to the stray-light contamination are the following:

- A fraction of the diffuse X-ray background outside the FoV is imaged inside the detector, increasing the background level over the entire sensitive area. This contamination is characterized by an azimuthal symmetry distribution over the focal plane detector.
- Point-like and extended sources outside the FoV could bring about an increasing of the background level. Such stray-light contamination will be only localized in a part of the detector and its intensity and spatial distribution will depend on the flux, energy spectra and off-axis angle of the contaminating source.

The effect of the stray-light becomes strongly penalizing when the telescope is observing sources at the very limit of its sensitivity and it reduces the telescope performance at higher energy where the fast decrease of the source flux produces statistically limited observations. The stray-light contamination has in such cases a strong impact that could severely compromise the scientific throughput.

The stray-light contamination can be quantified by the ratio of the total X-ray diffuse background focused onto the detector to the contribution coming from inside the FoV. This "stray-light contamination factor" ratio versus the focal plane detector radius is plotted in Fig. 1 where this ratio is also compared with SAX, JET-X and XMM. For the latter, the simulation was performed without the implementation of the pre-collimator X-ray baffle.^{14, 15} The stray-light contamination increases with the detector radius. However, this increase is particularly severe in Simbol-X up to a factor 2 at the edge of the FoV.

We also investigate different off-axis angles contributing to the stray-light. We have simulated diffuse background from annular regions at several angles and we have evaluated the contribution of each stray-light component (**N**, **P**, **H**) inside the focal plane detector. The stray-light is originated only from off-axis angles up to ~ 30 arcmin with a peak at ~ 15 arcmin off-axis (Fig. 2). Only **P** and **H** components contribute to the Simbol-X stray-light. There is no direct light (**N**).

The same results are obviously valid for point-like or extended sources outside the FoV.

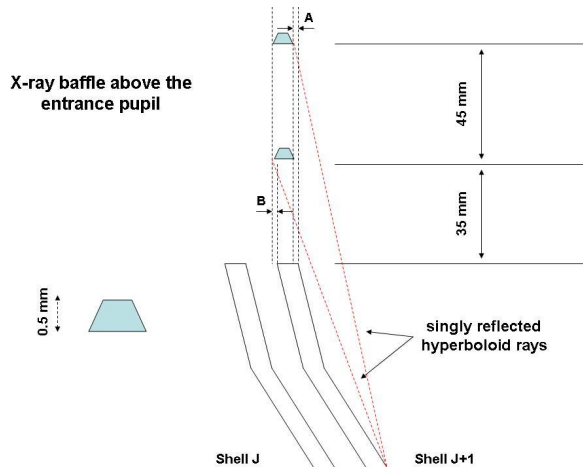


Figure 3. Sketch of the X-ray baffle above the Simbol-X entrance pupil: each mirror is equipped with a concentric ring which is set 35 mm above the entrance aperture and a second ring of equal shape, 45 mm above the first one. The inner radius (A) of each ring is larger than the inner radius of the mirror while the outer radius (B) could be slightly larger than the outer mirror radius (see sect. 4.1).

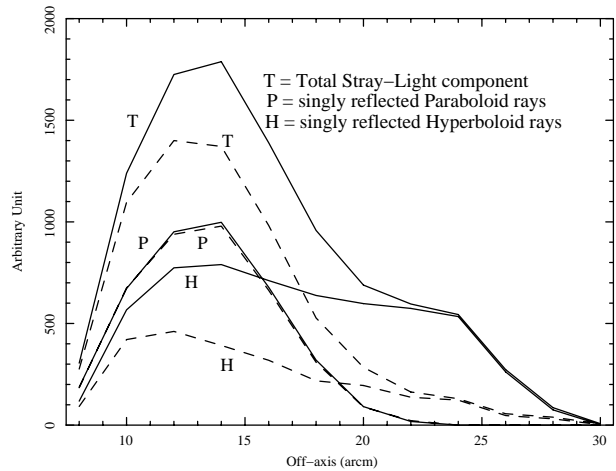


Figure 4. Stray-light originated from X-ray diffuse background emitted from annular regions out of the FoV versus off-axis angles. The total (T) and different contributions (P, H) are shown. Dashed lines show the residual stray-light contamination with an X-ray baffle above the entrance pupil (sect. 4.1)

4. X-RAY BAFFLE

The stray-light contamination in a X-ray telescope made of nested concentric mirrors could be strongly reduced if the radial distance between a mirror and the inner one were chosen at a proper value; the paraboloid surface of a mirror would therefore shade the on-axis photons on the entire hyperboloid surface of the adjacent outer mirror without shading the photons directed onto the paraboloid surface. Such a mirror configuration presents, on the other hand, some drawbacks:

- the FoV is reduced because the shadowing of a mirror onto the outer one increases very quickly with the off-axis angle
- the effective area changes compared to a telescope with the same number of mirrors and the same focal length but with larger gaps between the shells. The telescope will lose effective area at lower energies if mirrors are more tightly nested towards the optical axis while the telescope efficiency at higher energies will be strongly reduced if the mirrors are more tightly nested towards larger radii.

A good efficiency in stray-light reduction without the disadvantages proper of a telescope with more tightly nested mirrors could be achieved with the implementation of an X-ray baffle as for EINSTEIN, ROSAT and XMM telescopes.

Therefore, as clearly shown in Fig. 1, in order to achieve the maximum sensitivity foreseen for the Simbol-X optics design and to accomplish its foreseen scientific goals, the implementation of an X-ray baffle is mandatory.

The X-ray baffle should not only efficiently stop not only the unwanted stray-light but it should also not compromise the expected throughput for sources inside the FoV. We have studied three different X-ray baffle designs, have determined their efficiency and verified their impact on the Simbol-X performance.

4.1. X-ray baffle at the entrance pupil

A first design of X-ray baffle follows the baseline of the one already developed for the XMM telescope.^{14, 15} It consists of a complex X-ray baffle mounted above the entrance pupil of the telescope and accurately positioned

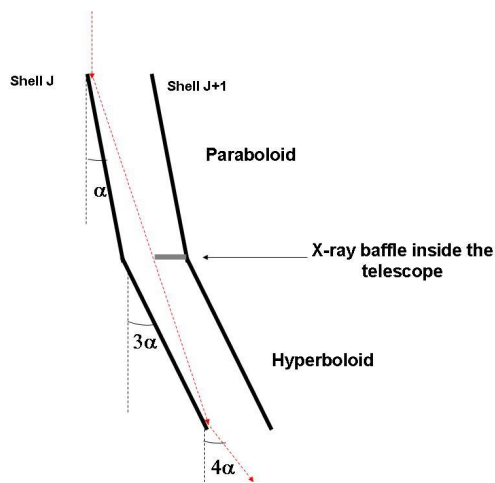


Figure 5. Sketch of the X-ray baffle inside the Simbol-X mirror structure: a circular rib leaning against the external wall of each mirror shell at the boundary between the paraboloid and the hyperboloid.

in front of the mirrors. A sketch of this baffle design is shown in Fig. 3. Each mirror is equipped with a concentric ring above the entrance aperture and a second ring of equal shape above the first one. *Singly reflected Hyperboloid rays* coming from a range of off-axis angles are stopped by the rings.

The ring height that optimizes the stray-light suppression varies from shell to shell depending on the slope of the mirror. In order to adopt a design having rings mounted at the same height for all shells, we derived the heights of the two sets of rings that minimize the stray-light contamination by using the raytracing code. The first rings plate is 35 mm above the entrance aperture while the second rings plate is 45 mm above the first one. To prevent on-axis effective area reduction due to an unwanted stopping of double reflection rays, the inner radius of each ring is 50 micron larger than the inner radius of the mirror. The outer radius of the ring could be slightly larger than the outer one of the mirror, with an excess, tuned for each ring, that maximizes the efficiency of the stray-light reduction without additional vignetting effect. In the optical axis direction each ring is 0.5 mm thick. Moreover, in order to avoid the optical stray-light due to the reflection on the surfaces parallel to the optical axis, we foresee, as in the XMM, to taper the inner and outer surface of the ring. The radial size of the rings varies between 0.3 mm and 0.1 mm while the separation between a ring and the adjacent one varies between 2.4 mm and 1.5 mm.

The X-ray baffle capability to block the two main stray-light components is shown in Fig 4: *singly reflected Hyperboloid rays* are largely suppressed while *singly reflected Paraboloid rays* are not blocked at all. The on-axis effective area of the telescope is not considerably modified by the presence of the baffle. The X-ray baffle produces a small vignetting at large off-axis: the maximum variation of the effective area at the boundary of the Simbol-X FoV is only 5% (Fig. 9 - dotted line).

4.2. X-ray baffle inside the telescope

EINSTEIN and ROSAT telescopes implemented an X-ray baffle inside the mirrors structure. The same type of baffle configuration is more difficult to implement in Simbol-X because of the limited space between the mirrors. Nevertheless, we have designed an "ad hoc" X-ray baffle inside the mirror structure: a circular rib leaning against the external wall of the mirror shell at the boundary between the paraboloid and the hyperboloid sections. The radial thickness of the rib is tuned for each mirror in order to prevent any stopping of the on-axis doubly reflected photons. The outer radius of a rib (Rm_j) will be equal to the minimum approaching distance between the path of a doubly reflected photon along its course through the mirror shells and the external surface of the inner

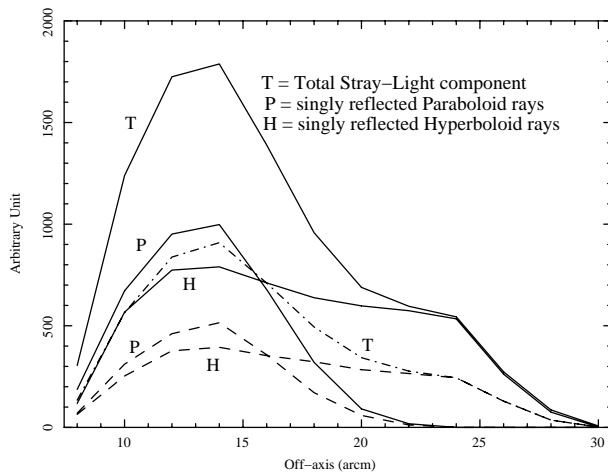


Figure 6. Stray-light originated from X-ray diffuse background emitted from annular regions out of the FoV versus off-axis angles. The total (**T**) and different contributions (**P**, **H**) are shown. Dashed lines show the residual stray-light contamination with an X-ray baffle inside the telescope (sect. 4.2)

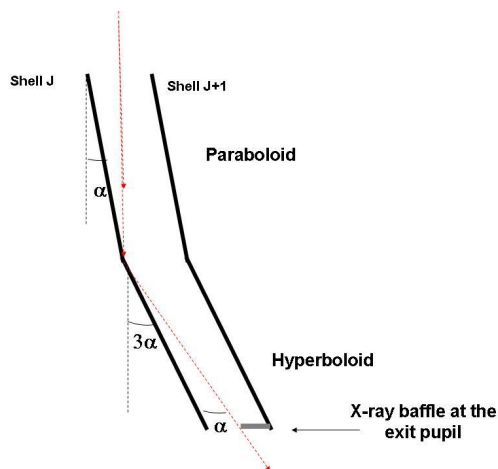


Figure 7. Sketch of the exit pupil X-ray baffle: a sieve plate made out of 99 circular rings, each in line with the bottom face of a mirror. The baffle could be included in the 24 arms spider structure at the bottom of the telescope.

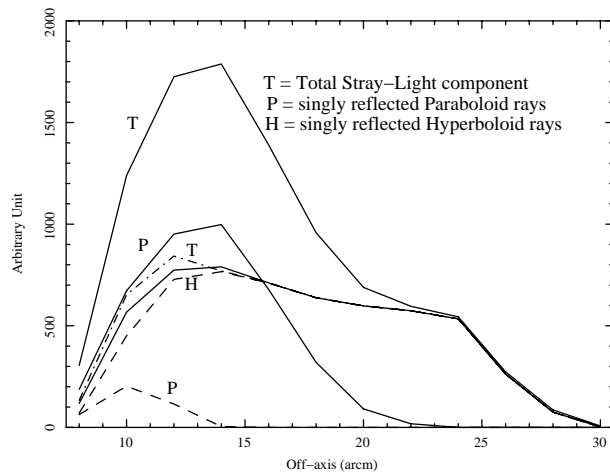


Figure 8. Stray-light originated from X-ray diffuse background emitted from annular regions out of the FoV versus off-axis angles. The total (**T**) and different contributions (**P**, **H**) are shown. Dashed lines show the residual stray-light contamination with an X-ray baffle at the exit pupil (sect. 4.1)

mirror at the paraboloid-hyperboloid boundary. As it is shown in Fig. 5 this requirement can be satisfied by avoiding to put obstacles to photons with the first reflection just on top of the paraboloid section. The radial thickness of the ribs is about 0.8 mm. As shown in Fig. 6 the baffle within the mirror structure significantly stops both the *singly reflected Paraboloid* and the *singly reflected Hyperboloid rays*. It does not produce any additional vignetting along the entire FoV (Fig. 9 - solid line).

4.3. X-ray baffle at the exit pupil

The third design of a Simbol-X X-ray baffle is located at the exit pupil of the telescope: a sieve plate made out of 99 circular rings, each in line with the bottom face of the mirrors. The geometrical principle of this baffle is shown in Fig. 7: on-axis photons, hitting the mirror $N = J$ ($J=1,99$) and crossing the telescope exit pupil, can approach a minimum distance ($Rmin_j$) to the external surface of the adjacent inner mirror $N = J + 1$ when they undergo a double reflection at the boundary between the paraboloid and the hyperboloid. In order to prevent on-axis effective area reduction we have, therefore, designed the outer radius of the $J + 1$ ring equal to $Rmin_j$ and its inner radius 50 micron larger than the inner radius of the mirror $J + 1$. The radial thickness of the rings varies between 1.1 mm and 0.8 mm. This X-ray baffle, in contact with the mirrors bottom face, could be included in the 24 arms spider structure at the bottom of the telescope.

The efficiency of the X-ray baffle is shown in Fig. 8: the *singly reflected Paraboloid rays* are largely blocked while only a small percentage of the *singly reflected Hyperboloid rays* are stopped. The X-ray baffle produces a monotonic increasing of the vignetting along the FoV with a maximum decrease of the effective area of 20% (Fig. 9 - dashed line).

5. CONCLUSION

In telescopes based on grazing incident mirrors not all photons undergo, in their path through the optics, a focusing double reflection. A significant percentage of photons from point-like sources and/or from diffuse X-ray light outside the telescope FoV may arrive at the focal plane with a single reflection or without any reflection at all, causing an increasing of the background level and limiting the telescope performance for faint and/or extended sources.

The stray-light contamination is more severe in Simbol-X than in previous telescopes because of the small mirror slopes coupled with large gaps between a shell and the adjacent one. Three different X-ray baffles,

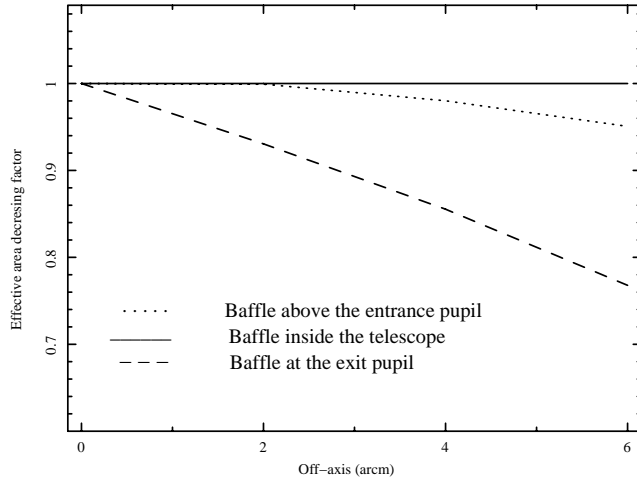


Figure 9. The ratio of the effective area obtained without an X-ray baffle to the effective area with the implementation of the baffle. Dotted line, solid line and dashed line correspond to the X-ray baffle above the entrance pupil, to the one inside the telescope structure and at the exit pupil, respectively.

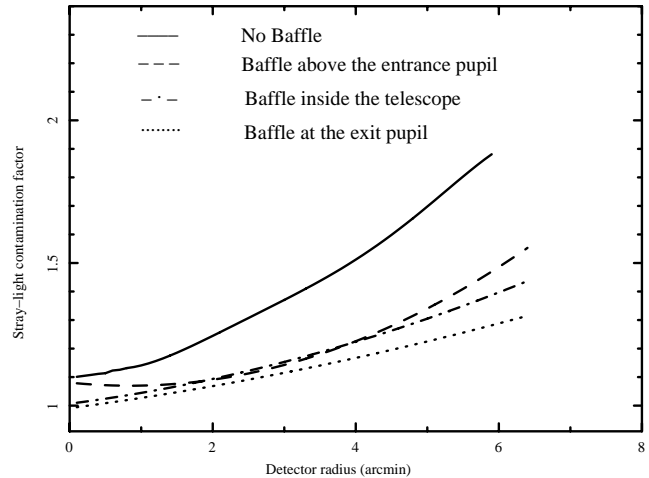


Figure 10. The "stray-light contamination factor" versus the focal plane radius. It represents the ratio of the X-ray diffuse background focused onto the detector to the contribution coming from the FoV only. The "stray-light contamination factor" for the different X-ray baffles is shown.

dedicated to the stray-light reduction, have been investigated. The stray-light stopping efficiency and the impact in the telescope performance have been verified by a raytracing code dedicated to the simulation of the Simbol-X optics.

- an X-ray baffle above the entrance pupil blocks a significant fraction of the *singly reflected Hyperboloid rays* but it is inefficient for the *singly reflected Paraboloid rays*. The X-ray baffle produces a very small additional vignetting at large off-axis: the maximum variation of the effective area at the boundary of the Simbol-X FoV is only 5%
- an X-ray baffle inside the telescope significantly reduces both the stray-light due to the *singly reflected Paraboloid rays* and the *singly reflected Hyperboloid rays*. The baffle does not produce any additional vignetting along the entire FoV
- an X-ray baffle at the exit pupil blocks a high percentage of the *singly reflected paraboloid rays* but it is totally inefficient to stop the *singly reflected hyperboloid rays*. The baffle produces a monotonic increase of the vignetting across the FoV with a maximum decrease of the effective area of 20%.

The efficiency of these X-ray baffles is summarized in Fig. 10: the diffuse X-ray background that is imaged, because of the stray-light, on the focal plane detector is significantly reduced and the "stray-light contamination factor" becomes similar to other X-ray telescopes.

REFERENCES

1. R. Giacconi, J. Bechtold, G. Branduardi, W. Forman, J. P. Henry, C. Jones, E. Kellogg, H. van der Laan, W. Liller, H. Marshall, S. S. Murray, J. Pye, E. Schreier, W. L. W. Sargent, F. Seward, and H. Tananbaum, "A high-sensitivity X-ray survey using the Einstein Observatory and the discrete source contribution to the extragalactic X-ray background," *ApJ Letters* **234**, pp. L1–L7, Nov. 1979.
2. J. Truemper, "The ROSAT mission," *Advances in Space Research* **2**, pp. 241–249, 1982.
3. G. Boella, L. Chiappetti, G. Conti, G. Cusumano, S. del Sordo, G. La Rosa, M. C. Maccarone, T. Mineo, S. Molendi, S. Re, B. Sacco, and M. Tripiciano, "The medium-energy concentrator spectrometer on board the BeppoSAX X-ray astronomy satellite," *A&A Suppl.* **122**, pp. 327–340, Apr. 1997.

4. Y. Tanaka, H. Inoue, and S. S. Holt, "The X-ray astronomy satellite ASCA," *PASJ* **46**, pp. L37–L41, June 1994.
5. B. Aschenbach, U. G. Briel, F. Haberl, H. W. Braeuninger, W. Burkert, A. Oppitz, P. Gondoin, and D. H. Lumb, "Imaging performance of the XMM-Newton x-ray telescopes," in *Proc. SPIE Vol. 4012, p. 731-739, X-Ray Optics, Instruments, and Missions III, Joachim E. Truemper; Bernd Aschenbach; Eds., J. E. Truemper and B. Aschenbach, eds., pp. 731–739, July 2000.*
6. M. C. Weisskopf, H. D. Tananbaum, L. P. Van Speybroeck, and S. L. O'Dell, "Chandra X-ray Observatory (CXO): overview," in *Proc. SPIE Vol. 4012, p. 2-16, X-Ray Optics, Instruments, and Missions III, Joachim E. Truemper; Bernd Aschenbach; Eds., J. E. Truemper and B. Aschenbach, eds., pp. 2–16, July 2000.*
7. N. Gehrels, G. Chincarini, P. Giommi, K. O. Mason, J. A. Nousek, A. A. Wells, N. E. White, S. D. Barthelmy, D. N. Burrows, L. R. Cominsky, K. C. Hurley, F. E. Marshall, P. Mészáros, P. W. A. Roming, L. Angelini, L. M. Barbier, T. Belloni, S. Campana, P. A. Caraveo, M. M. Chester, O. Citterio, T. L. Cline, M. S. Cropper, J. R. Cummings, A. J. Dean, E. D. Feigelson, E. E. Fenimore, D. A. Frail, A. S. Fruchter, G. P. Garmire, K. Gendreau, G. Ghisellini, J. Greiner, J. E. Hill, S. D. Hunsberger, H. A. Krimm, S. R. Kulkarni, P. Kumar, F. Lebrun, N. M. Lloyd-Ronning, C. B. Markwardt, B. J. Mattson, R. F. Mushotzky, J. P. Norris, J. Osborne, B. Paczynski, D. M. Palmer, H.-S. Park, A. M. Parsons, J. Paul, M. J. Rees, C. S. Reynolds, J. E. Rhoads, T. P. Sasseen, B. E. Schaefer, A. T. Short, A. P. Smale, I. A. Smith, L. Stella, G. Tagliaferri, T. Takahashi, M. Tashiro, L. K. Townsley, J. Tueller, M. J. L. Turner, M. Vietri, W. Voges, M. J. Ward, R. Willingale, F. M. Zerbi, and W. W. Zhang, "The Swift Gamma-Ray Burst Mission," *ApJ* **611**, pp. 1005–1020, Aug. 2004.
8. H. Kunieda and Suzaku Team, "Mission overview of Suzaku and topics of observations," *American Astronomical Society Meeting Abstracts* **207**, pp. –+, Dec. 2005.
9. G. K. Skinner, "Coded-Mask Imaging in Gamma-Ray Astronomy - Separating the Real and Imaginary parts of a Complex subject," *ArXiv Astrophysics e-prints*, Feb. 2003.
10. C. Winkler, T. J.-L. Courvoisier, G. Di Cocco, N. Gehrels, A. Giménez, S. Grebenev, W. Hermsen, J. M. Mas-Hesse, F. Lebrun, N. Lund, G. G. C. Palumbo, J. Paul, J.-P. Roques, H. Schnopper, V. Schönfelder, R. Sunyaev, B. Teegarden, P. Ubertini, G. Vedrenne, and A. J. Dean, "The INTEGRAL mission," *A&A* **411**, pp. L1–L6, Nov. 2003.
11. P. Ferrando, A. Goldwurm, P. Laurent, O. Limousin, J. Martignac, F. Pinsard, Y. Rio, J. P. Roques, O. Citterio, G. Pareschi, G. Tagliaferri, F. Fiore, G. Malaguti, U. Briel, G. Hasinger, and L. Strüder, "SIMBOL-X: a formation flying mission for hard-x-ray astrophysics," in *Optics for EUV, X-Ray, and Gamma-Ray Astronomy II. Edited by Citterio, Oberto; O'Dell, Stephen L. Proceedings of the SPIE, Volume 5900, pp. 195-204 (2005).*, O. Citterio and S. L. O'Dell, eds., pp. 195–204, Aug. 2005.
12. G. Pareschi, S. Basso, O. Citterio, M. Ghigo, F. Mazzoleni, D. Spiga, W. Burkert, M. Freyberg, G. D. Hartner, G. Conti, E. Mattaini, G. Grisoni, G. Valsecchi, B. Negri, G. Parodi, A. Marzorati, and P. dell'Acqua, "Development of grazing-incidence multilayer mirrors by direct Ni electroforming replication: a status report," in *Optics for EUV, X-Ray, and Gamma-Ray Astronomy II. Edited by Citterio, Oberto; O'Dell, Stephen L. Proceedings of the SPIE, Volume 5900, pp. 47-58 (2005).*, O. Citterio and S. L. O'Dell, eds., pp. 47–58, Aug. 2005.
13. P. Ferrando, M. Arnaud, B. Cordier, A. Goldwurm, O. Limousin, J. Paul, J. L. Sauvageot, P.-O. Petrucci, M. Mouchet, G. F. Bignami, O. Citterio, S. Campana, G. Pareschi, G. Tagliaferri, U. G. Briel, G. Hasinger, L. Strueder, P. Lechner, E. Kendziorra, and M. J. L. Turner, "SIMBOL-X: a new-generation hard x-ray telescope," in *Optics for EUV, X-Ray, and Gamma-Ray Astronomy. Edited by Citterio, Oberto; O'Dell, Stephen L. Proceedings of the SPIE, Volume 5168, pp. 65-76 (2004).*, O. Citterio and S. L. O'Dell, eds., pp. 65–76, Feb. 2004.
14. D. Chambure, R. Laine, K. Katwijk, W. Ruebe, A. Valenzuela, D. SchinK, E. Hoelzle, Y. Gutierrez, M. Domingo, I. Ibarrete, J. P. Tock, I. Domken, Y. Stockman, Y. Houbrecht, H. Hamsen, and B. Aschenbach, "The X-ray Baffle of the XMM Telescope: development and results," in *Proc. International Symposium of the Optical Design and Production - EUROPTO Series 1999 - Berlin (Germany) - Plenary Session, 1999.*

15. D. Chambure, R. Laine, K. Katwijk, P. Kletzki, A. Valenzuela, G. Grisomi, C. Canali, S. Hofer, S. P. Tock, I. Domken, Y. Stockman, H. Hamsen, M. Leonard, B. Aschembach, and H. Brauminger, "Lesson learnt from the development of the XMM Optics," in *Proc. International Symposium of the Optical Design and Production - EUROPTO Series 1999 - Berlin (Germany) - Plenary Session*, 1999.